ARTICLE

doi:10.1038/nature10926

Teneurins instruct synaptic partner matching in an olfactory map

Weizhe Hong[1], Timothy J. Mosca[1] & Liqun Luo[1]

Neurons are interconnected with extraordinary precision to assemble a functional nervous system. Compared to axon guidance, far less is understood about how individual pre- and postsynaptic partners are matched. To ensure the proper relay of olfactory information in the fruitfly *Drosophila*, axons of ~50 classes of olfactory receptor neurons (ORNs) form one-to-one connections with dendrites of ~50 classes of projection neurons (PNs). Here, using genetic screens, we identified two evolutionarily conserved, epidermal growth factor (EGF)-repeat containing transmembrane Teneurin proteins, Ten-m and Ten-a, as synaptic-partner-matching molecules between PN dendrites and ORN axons. Ten-m and Ten-a are highly expressed in select PN–ORN matching pairs. Teneurin loss- and gain-of-function cause specific mismatching of select ORNs and PNs. Finally, Teneurins promote homophilic interactions *in vitro*, and Ten-m co-expression in non-partner PNs and ORNs promotes their ectopic connections *in vivo*. We propose that Teneurins instruct matching specificity between synaptic partners through homophilic attraction.

The chemoaffinity hypothesis was proposed nearly 50 years ago to explain the target specificity of regenerating optic nerves: developing neurons "must carry individual identification tags, presumably cytochemical in nature, by which they are distinguished one from another almost, in many regions, to the level of the single neuron"[1]. Many molecules are now known that guide axons to their target areas[2,3], but few may mediate mutual selection and direct matching between individual pre- and postsynaptic partners. Here we show that the transmembrane Teneurin proteins instruct the selection of specific synaptic partners in the *Drosophila* olfactory circuit (Supplementary Fig. 1).

In *Drosophila*, individual classes of ORN axons make one-to-one connections with individual classes of second-order PN dendrites within one of ~50 discrete glomeruli in the antennal lobe. We refer to this specific one-to-one connection as PN–ORN synaptic partner matching. Olfactory circuit assembly takes place in sequential steps before sensory activity begins[4–6]. PN dendrites first elaborate within and pattern the developing antennal lobe[7–9], which is followed by invasion of ORN axons[10–14]. Importantly, re-positioning PN dendrites redirects their partner ORN axons without disrupting the connections[15], suggesting that proper PN–ORN connections probably involve direct recognition and matching between partners.

Matching screens identified Ten-m and Ten-a

To identify potential PN–ORN matching molecules, we simultaneously labelled select PN dendrites and ORN axons in two colours and performed two complementary genetic screens (Fig. 1a, d). We overexpressed 410 candidate cell-surface molecules, comprising ~40% of the potential cell-recognition molecules in *Drosophila*[16]. In the first screen, we used *Mz19-GAL4* to label DA1, VA1d and DC3 PNs (hereafter Mz19 PNs), and *Or47b-rCD2* to label Or47b ORNs (Fig. 1a, b). Or47b ORN axons normally project to the VA1lm glomerulus and are adjacent to Mz19 PN dendrites without overlap. We overexpressed candidate cell-surface molecules only in Mz19 PNs to identify those that promoted ectopic connections between Or47b axons and Mz19 dendrites (Fig. 1a). We found that overexpression of *ten-m* (*P{GS}9267*; Supplementary Fig. 2b) produced ectopic connections (Fig. 1c).

In the second screen, we labelled Mz19 PNs as above and Or88a ORNs using *Or88a-rCD2* (Fig. 1d, e). Or88a ORN axons normally project to the VA1d glomerulus, intermingling extensively with VA1d PN dendrites (Fig. 1e). We overexpressed candidate cell-surface molecules in Mz19 PNs (Fig. 1d) as above and found that overexpression of *ten-a* (*P{GE}1914*, Supplementary Fig. 2a) partially disrupted the intermingling of Or88a axons and Mz19 dendrites (Fig. 1f).

In addition to impairing PN–ORN matching, *ten-m* and *ten-a* overexpression shifted Mz19 PN dendrite position (Fig. 1c, f). However, mismatching was not a secondary consequence of axon or dendrite mispositioning; mispositioning alone, caused by perturbation of other genes, does not alter PN–ORN matching[9,13,15]. Furthermore, among 410 candidate molecules, only *ten-m* and *ten-a* overexpression exhibited mismatching defects, suggesting their specificity in PN–ORN matching.

Both *ten-m* and *ten-a* appear to encode type II transmembrane proteins[17–19]. They possess highly similar domain compositions and amino acid sequences; each contains eight EGF-like and multiple YD (tyrosine-aspartate) repeats within its large carboxy-terminal extracellular domain (Fig. 1g). Ten-m and Ten-a were initially identified as tenascin-like molecules[20,21], but vertebrate teneurins were later identified as their true homologues based on sequence and domain similarity (Fig. 1h). Thus, we refer to Ten-m and Ten-a as *Drosophila* Teneurins. Teneurins are present in nematodes, flies and vertebrates. In human, teneurin-1 and teneurin-2 are located in chromosomal regions associated with intellectual disability[17], and teneurin-4 is linked to susceptibility to bipolar disorder[22].

Drosophila ten-m was originally identified as a pair-rule gene required for embryonic patterning[21,23], but this function was recently shown to be unrelated to *ten-m*[24]. Teneurins were implicated in synapse development at the neuromuscular junction[16,25] (see ref. 26), and Ten-m also regulates motor axon guidance[24]. Neither the underlying mechanisms nor their potential roles in the central nervous system are known. Vertebrate teneurins are widely expressed in the nervous system[18,27] and interact homophilically *in vitro*[28,29], suggesting their potential role as homophilic cell adhesion molecules in patterning neuronal connectivity.

[1]Department of Biology, Howard Hughes Medical Institute, Stanford University, Stanford, California 94305, USA.

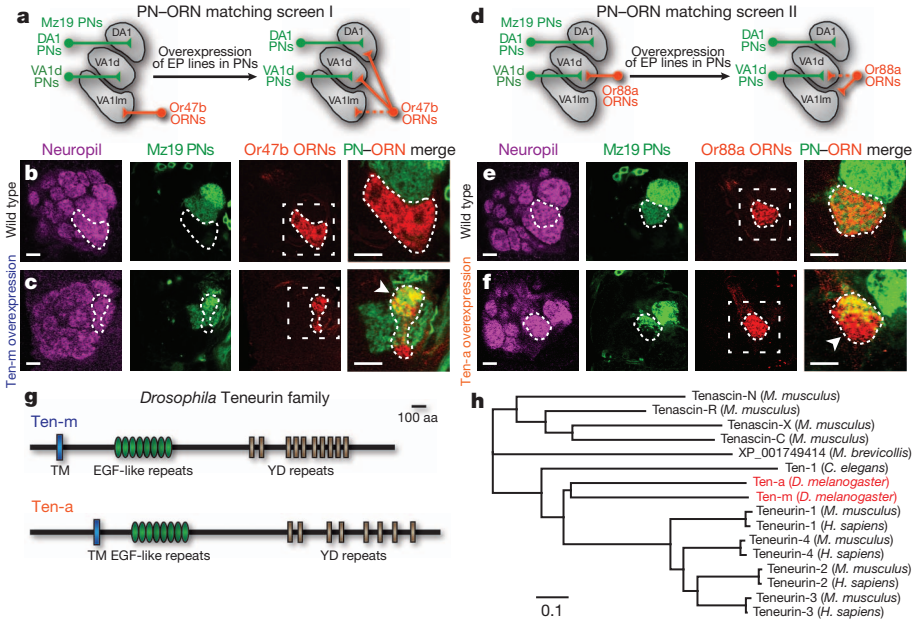

Figure 1 | PN–ORN synaptic matching screens identify two Teneurins. **a**, **d**, Schematics showing two PN–ORN matching screens. PN dendrites are labelled by *Mz19-GAL4* driving mCD8GFP and ORN axons by *Or47b-rCD2* (**a**) or *Or88a-rCD2* (**d**). Each EP line has a transposable element insertion that places *UAS* 5′ to a gene encoding a predicted cell-surface protein, which can be overexpressed using *Mz19-GAL4*. **b**, **c**, Or47b axons and Mz19 dendrites do not overlap in control (**b**), but form ectopic connections following Ten-m overexpression (**c**), as seen by axon-dendrite intermingling (arrowhead). **e**, **f**, Or88a axons and Mz19 dendrites connect at the VA1d glomerulus in control (**e**), but the connection is partially lost following Ten-a overexpression, as some of the Or88a axons no longer intermingle with Mz19 dendrites (arrowhead). Target areas of Or47b (**b**, **c**) or Or88a (**e**, **f**) axons are outlined. Mismatching phenotypes are quantified in Supplementary Figs 9k and 10q. The first three columns in **b**, **c**, **e**, **f** show separate channels of the same section; the fourth shows higher magnification of the dashed squares (as in Figs 3, 4, 5d–g.). Unless indicated, all images in this and subsequent figures are single confocal sections and all scale bars are 10 μm. **g**, Domain composition of *Drosophila* Ten-m and Ten-a. aa, amino acids; TM, transmembrane domain. **h**, Phylogeny of the *Drosophila* Teneurins and related proteins in other species. Branch lengths represent units of substitutions per site of the sequence alignment. Teneurins are evolutionarily conserved in bilaterians and a unicellular choanoflagellate *Monosiga brevicollis*, but not in cnidarians.

Matching expression of Ten-m and Ten-a

Both *Drosophila* Teneurin proteins were endogenously expressed in the developing antennal lobe (Fig. 2a and Supplementary Fig. 3). At 48 h after puparium formation (APF), when individual glomeruli just become identifiable, elevated Teneurin expression was evident in select glomeruli. The subset of glomeruli expressing elevated Ten-m was distinct but partially overlapping with that expressing elevated Ten-a (Fig. 2a, e). Teneurin proteins were also detected at a low level in all glomeruli. Both basal and elevated Teneurin expressions were eliminated by pan-neuronal RNA interference (RNAi) targeting the corresponding gene (Fig. 2b, c), suggesting that Teneurin proteins are produced predominantly by neurons. In a *ten-a* null mutant we generated (Supplementary Fig. 2a), all Ten-a expression was eliminated, confirming antibody specificity (Fig. 2d).

The antennal lobe consists of ORN axons as well as PN and local interneuron dendrites. We used intersectional analysis to determine the cellular source for elevated Teneurin expression. For *ten-m*, we screened GAL4 enhancer traps near the *ten-m* gene, and identified NP6658 (hereafter *ten-m-GAL4*; Supplementary Fig. 2b) that recapitulated the glomerulus-specific Ten-m staining pattern (Supplementary Fig. 4a–c). We used a FLPout reporter *UAS>stop>mCD8GFP* to determine the intersection of *ten-m-GAL4* and an ORN-specific *ey-Flp* (Fig. 2f and Supplementary Fig. 4d–f) or a PN-specific *GH146-Flp* (Fig. 2g and Supplementary Fig. 4g–i). We found that *ten-m-GAL4* was selectively expressed in a subset of ORNs and PNs. Owing to reagent availability, we focused our analysis on five glomeruli (DA1, VA1d, VA1lm, DC3 and DA3), adjacently located on the lateral and anterior side of the antennal lobe. In these five glomeruli, Ten-m expression in PN and ORN classes matched: high levels in PNs corresponded to high levels in ORNs and vice versa (Fig. 2f, g).

To determine the cellular origin of elevated Ten-a expression, we performed tissue-specific RNAi of endogenous Ten-a, as no GAL4 enhancer trap is available near *ten-a*. To isolate Ten-a expression in ORNs, we drove pan-neuronal *ten-a* RNAi while specifically suppressing RNAi in ORNs using *tubP>stop>GAL80* and *ey-Flp* (Fig. 2h). To restrict Ten-a expression to central neurons, we expressed *ten-a* RNAi in all ORNs (Fig. 2i). We found that Ten-a was highly expressed in a subset of ORNs and central neurons, and also showed a matching expression in the five glomeruli we focused on (Fig. 2h, i). The glomerular-specific differential Ten-a expression in central neurons probably arises mainly from PNs as they target dendrites to specific glomeruli, and punctate Ten-a staining was observed in PN cell bodies (Supplementary Fig. 5). In summary, Ten-m and Ten-a are each highly expressed in a distinct, but partially overlapping, subset of matching ORNs and PNs (Fig. 2j).

Teneurins are required for PN–ORN matching

To examine whether Teneurins are required for proper PN–ORN matching, we performed tissue-specific RNAi (Fig. 3 and Supplementary Fig. 2c) in all neurons using *C155-GAL4*, in PNs using *GH146-GAL4*, or in ORNs using *peb-GAL4*. To label specific subsets of PN dendrites independent of GAL4-UAS, we used the Q binary expression system[30], and converted *Mz19-GAL4* to *Mz19-QF* by bacterial artificial chromosome (BAC) recombineering (Supplementary Fig. 2d). We could thus perform GAL4-based RNAi knockdown while labelling PN dendrites and ORN axons in two colours independent of GAL4. We focused our analysis on Mz19 dendrites and Or47b axons, which innervate neighbouring glomeruli but never intermingle in wild type (Figs 1b and 3a, b).

Pan-neuronal RNAi of both *teneurin* genes shifted Or47b axons to a position between two adjacent Mz19 glomeruli, DA1 and VA1d (Fig. 3c). Moreover, Mz19 dendrites and Or47b axons intermingled without a clear border (Fig. 3c, d), reflecting a PN–ORN matching defect. We confirmed this using independent RNAi lines targeting

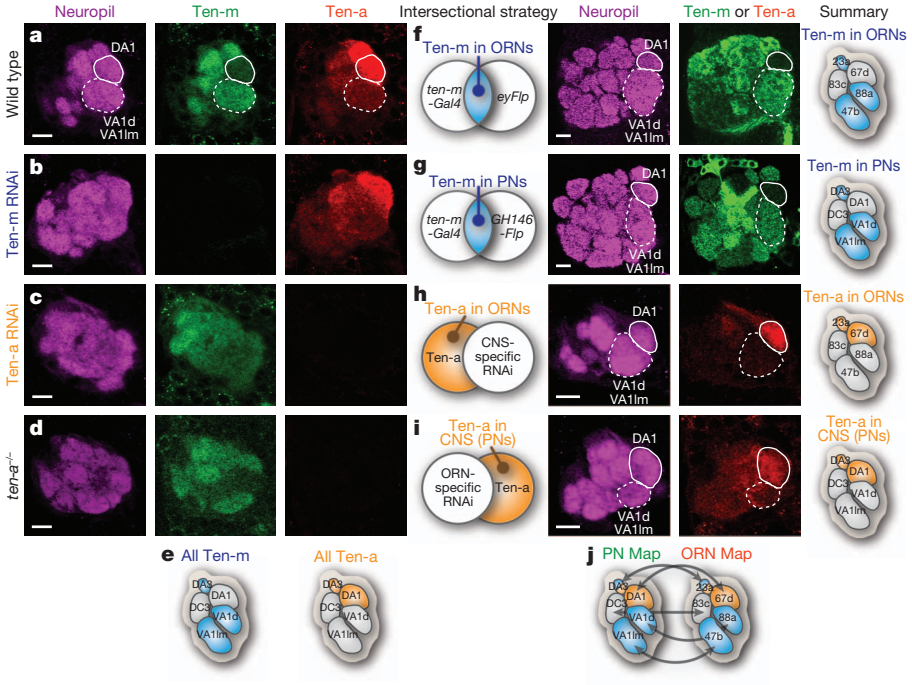

Figure 2 | Ten-m and Ten-a are differentially expressed in matching PN and ORN classes. **a**, Developing antennal lobes at 48 h APF stained by antibodies against Ten-m, Ten-a, and a neuropil marker, N-cadherin. Solid lines encircle the DA1 glomerulus (Ten-m low, Ten-a high). Dashed lines encircle the VA1d/VA1lm glomeruli (Ten-m high, Ten-a low). **b**, **c**, Ten-m and Ten-a proteins are undetectable following pan-neuronal RNAi of *ten-m* (**b**) and *ten-a* (**c**), respectively. **d**, A *ten-a* homozygous mutant eliminated the Ten-a antibody staining. **e**, Summary of elevated Ten-m and Ten-a expression in five select glomeruli. **f**, **g**, Expression of the Flp-out GFP reporter *UAS>stop>mCD8GFP* at the intersection of *ten-m-GAL4* with ORN-specific *ey-Flp* (**f**) or with PN-specific *GH146-Flp* (**g**) in adult. **h**, **i**, Antibody staining of Ten-a in central nervous system (CNS)-neuron-specific RNAi (**h**) or in ORN-specific RNAi (**i**) at 48 h APF. **f**–**i**, Right, individual cell-type-specific Teneurin expression patterns are schematically summarized. **j**, Combined expression patterns of Teneurin proteins in PNs (left) and ORNs (right). Blue, Ten-m high; orange, Ten-a high. Scale bars, 10 μm.

different regions of the *ten-m* and *ten-a* transcripts (Supplementary Fig. 6). Further, knocking down *ten-m* and *ten-a* only in PNs or only in ORNs also led to Mz19–Or47b intermingling (Fig. 3e and Supplementary Fig. 7a, d), indicating that Teneurins are required in both PNs and ORNs to ensure proper matching.

Next, we examined the contribution of each Teneurin by individual RNAi knockdown in ORNs. Knocking down *ten-m* and, to a lesser extent, *ten-a*, caused mild mismatching (Fig. 3e and Supplementary Fig. 7). This was greatly enhanced by simultaneous knockdown of both *ten-m* and *ten-a* (Fig. 3e), probably because Mz19–Or47b

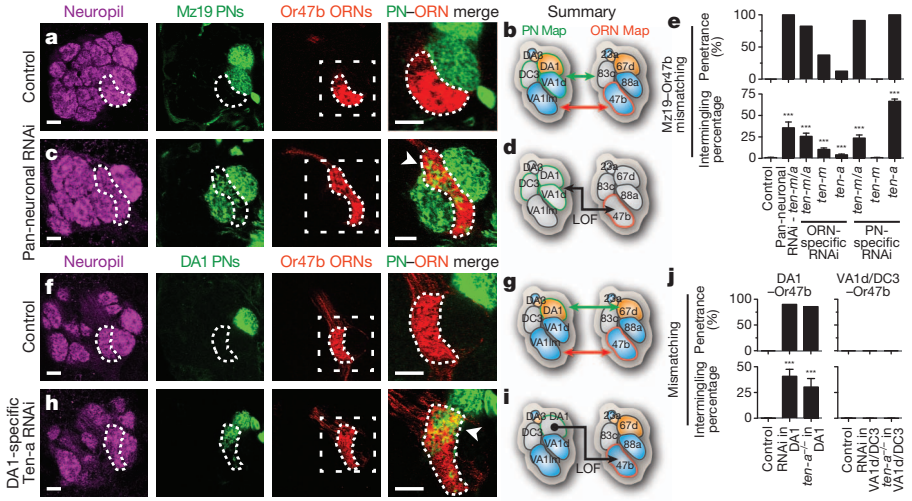

Figure 3 | Loss of Teneurins causes PN–ORN mismatching. **a**, Normally, Mz19 dendrites (green) innervate glomeruli adjacent to the VA1lm glomerulus, which is itself innervated by Or47b axons (red). The dashed line encircles Or47b axons. DC3 PNs are located posterior to DA1/VA1d PNs and Or47b ORNs, and are not visible in these sections. **c**, Mismatching phenotypes in *ten-m* and *ten-a* RNAi driven by the pan-neuronal driver *C155-GAL4*. Dashed lines encircle Or47b ORN axons, showing intermingling with Mz19 PN dendrites (arrowhead). **e**, Quantification of Mz19–Or47b mismatching phenotypes. For all genotypes, $n \geq 15$. **f**, In control, DA1 PNs do not intermingle with Or47b ORNs. **h**, MARCM expression of *ten-a* RNAi in DA1 PNs causes dendrite intermingling with Or47b axons (arrowhead). **j**, Quantification of mismatching phenotypes. For all genotypes, $n \geq 6$. Error bars represent s.e.m. ***, $P < 0.001$ compared to control. **b**, **d**, **g**, **i**, Summary showing normal connectivity in control (**a**, **f**) and mismatching phenotypes following *teneurin* RNAi (**c**, **h**). Blue, Ten-m high; orange, Ten-a high. Green outlines, labelled PNs. Red outlines, labelled ORNs. Scale bars, 10 μm.

mismatching requires weakening connections with their respective endogenous partners (Supplementary Fig. 7g). This synergy implies that multiple matching molecules can enhance partner matching robustness.

We also tested the functions of individual Teneurins in PNs. We found that the Mz19–Or47b mismatching was caused by PN-specific knockdown of *ten-a*, but not *ten-m* (Fig. 3e and Supplementary Fig. 7). As VA1d/DC3 and DA1 PNs arise from separate neuroblast lineages[31], we used mosaic analysis with a repressible cell marker (MARCM) to generate neuroblast clones to label and knockdown *ten-a* in DA1 or VA1d/DC3 PNs (Fig. 3f–j; see Methods). *ten-a* knockdown only in DA1 PNs (normally Ten-a high) caused their dendrites to mismatch with Or47b axons (Fig. 3h–j). By contrast, *ten-a* knockdown in VA1d/DC3 PNs (normally Ten-a low) did not cause mismatching (Fig. 3j and Supplementary Fig. 8a, b). Similarly, MARCM loss-of-function of *ten-a* mutant in DA1 but not in VA1d/DC3 PNs resulted in mismatching with Or47b ORNs (Fig. 3j and Supplementary Fig. 8c, d). Thus, removal of *ten-a* from Ten-a-high DA1 PNs caused their dendrites to mismatch with Ten-a-low Or47b ORNs (Fig. 3i). The differential requirements of Ten-m and Ten-a in ORNs or PNs in preventing Mz19–Or47b mismatching probably reflect differential expression of Ten-m and Ten-a in the mismatching partners.

Our finding that loss of *ten-a* caused Ten-a-high PNs to mismatch with Ten-a-low ORNs (Fig. 3i, j), together with the matching expression of Teneurin proteins in PNs and ORNs, raised the possibility that Teneurins instruct class-specific PN–ORN connections through homophilic attraction: PNs expressing high-level Ten-m or Ten-a connect to ORNs with high-level Ten-m or Ten-a, respectively.

Teneurins instruct matching specificity

This homophilic attraction hypothesis predicts that overexpression of a given Teneurin in PNs (1) should preferentially affect PNs normally expressing low levels of that Teneurin, causing their dendrites to lose endogenous connections with their cognate ORNs, and (2) should cause these PNs to make ectopic connections with ORNs expressing high levels of that Teneurin.

To test the first prediction, we examined whether Teneurin overexpression in Mz19 PNs impaired their endogenous connections with cognate ORNs. Consistent with our prediction, Ten-m overexpression specifically disrupted the connections of DA1 PNs and Or67d ORNs, a PN–ORN pair expressing low-level Ten-m (Supplementary Fig. 9b, e). Connections of the other two pairs were unaffected (Supplementary Fig. 9a, c, d, f). Likewise, Ten-a overexpression specifically disrupted connections between VA1d PNs and Or88a ORNs, a PN–ORN pair expressing low-level Ten-a (Supplementary Fig. 9g), but not between the other two PN–ORN pairs (Supplementary Fig. 9h, i).

To test the second prediction, we examined the specificity of ectopic connections made by Mz19 PNs overexpressing Teneurins, and sampled five non-partner ORN classes that project axons to the vicinity of Mz19 dendrites (Supplementary Fig. 10). We found that Ten-m overexpression in Mz19 PNs caused their dendrites to mismatch only with Or47b ORNs (Supplementary Fig. 10f). To examine additional mismatching phenotypes that may occur within Mz19 glomeruli and to determine whether DA1 or VA1d/DC3 PNs contribute to the ectopic connections, we used MARCM to overexpress Ten-m in individual PN classes. We found that Ten-m overexpression in DA1 PNs (Ten-m low) caused their dendrites to mismatch with Or47b (Fig. 4a, b) and (to a lesser extent) Or88a ORNs (Fig. 4b, c), both endogenously expressing high-level Ten-m. By contrast, Ten-m overexpression in VA1d/DC3 PNs did not produce ectopic connections with any non-matching ORNs tested (Fig. 4d–f).

Likewise, Ten-a overexpression in Mz19 PNs caused their dendrites to mismatch only with Or23a ORNs among all non-matching ORN classes sampled outside the Mz19 region (Supplementary Fig. 10l).

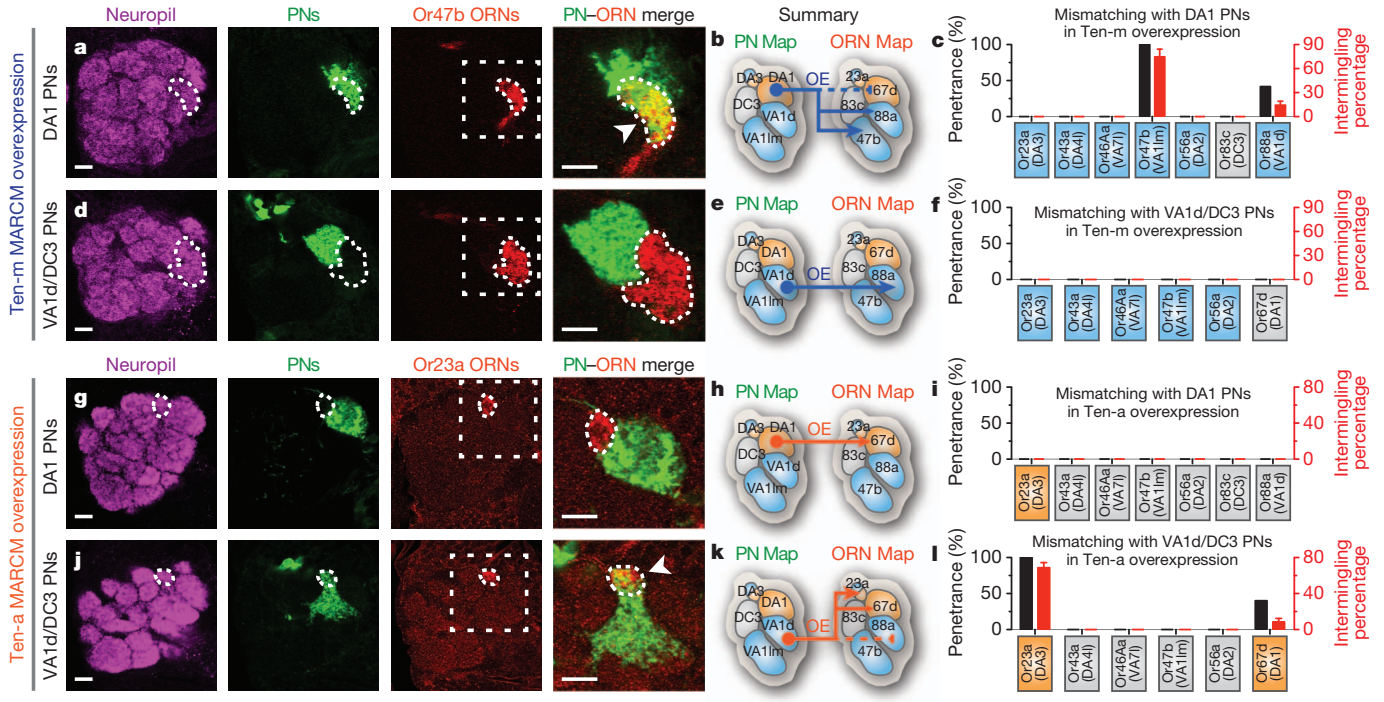

Figure 4 | Teneurin overexpression in specific PN classes causes mismatching. **a**–**l**, Mismatching phenotypes following Ten-m (**a**–**f**) or Ten-a (**g**–**l**) overexpression in different PN classes. Specific PN classes are labelled by MARCM with *Mz19-GAL4* and ORN axons using *Or47b-rCD2* (**a**, **d**) or *Or23a-mCD8GFP* (**g**, **j**). In control, Mz19 PNs do not intermingle with Or47b ORNs (Fig. 1b). MARCM overexpression of Ten-m in DA1 PNs (**a**, arrowhead), but not VA1d/DC3 PNs (**d**), causes dendrite mismatching with Or47b axons. MARCM overexpression of Ten-a in VA1d/DC3 PNs (**j**, arrowhead), but not in DA1 PNs (**g**), causes their dendrites to mismatch with Or23a axons. *P{GS}9267* and *P{GE}1914* (Supplementary Fig. 2) are used to overexpress Ten-m and Ten-a, respectively. **c**, **f**, **i**, **l**, Quantification of mismatching phenotypes ($n = 9$ for each). Error bars represent s.e.m. See Supplementary Fig. 10 for details on some genotypes quantified here. **b**, **e**, **h**, **k**, Schematic summarizing the mismatching phenotypes in Fig. 4 and Supplementary Figs 9 and 10. Blue, Ten-m high; orange, Ten-a high. Scale bars, 10 μm.

Further, MARCM overexpression of Ten-a in VA1d/DC3 PNs (Ten-a low) caused their dendrites to mismatch specifically with Or23a (Fig. 4j, k) and (to a lesser extent) Or67d ORNs (Fig. 4k, l), both endogenously expressing high-level Ten-a (Fig. 4l). By contrast, Ten-a overexpression in DA1 PNs (Ten-a high) did not produce ectopic connections with any non-matching ORNs tested (Fig. 4g–i). Thus, both Ten-m and Ten-a overexpression analyses support the homophilic attraction hypothesis.

Our data also suggest that additional molecule(s) are required to determine completely the wiring specificity of the five PN–ORN pairs examined. For example, VA1d–Or88a and VA1lm–Or47b have indistinguishable Ten-m/Ten-a expression patterns (Fig. 2j), and may require additional molecules to distinguish target choice. Indeed, Ten-a knockdown (Fig. 3h–j and Supplementary Fig. 8e, f) or Ten-m overexpression (Fig. 4b, c) caused DA1 PNs to mismatch preferentially with Or47b as opposed to Or88a axons. This suggests that the non-adjacent DA1 and VA1lm share a more similar Teneurin-independent cell-surface code than the adjacent VA1d and VA1lm. Likewise, Ten-a overexpression caused VA1d PNs to mismatch with the non-adjacent Or23a more so than the adjacent Or67d ORNs, even though both ORNs express high-level Ten-a (Fig. 4k, l). Finally, Ten-m overexpression in DC3 PNs, which express low-level Ten-m, did not change its matching specificity (Fig. 4f and Supplementary Fig. 9f), suggesting that Teneurin-independent mechanisms are involved in matching DC3 PNs and Or83c ORNs.

In summary, we showed that Teneurin overexpression in Teneurin-low PNs caused their dendrites to lose endogenous connections with Teneurin-low ORNs and mismatch with Teneurin-high ORNs (Fig. 4b, k). However, Teneurin overexpression in Teneurin-high PNs did not disrupt their proper connections (Fig. 4e, h). These data indicate that Teneurins instruct connection specificity, probably through homophilic attraction, by matching Ten-m or Ten-a levels in PN and ORN partners.

Ten-m promotes PN–ORN homophilic attractions

To test whether Teneurins interact *in vitro*, we separately transfected two populations of *Drosophila* S2 cells with Flag- and haemagglutinin (HA)-tagged Teneurins, and performed co-immunoprecipitations from lysates of these cells after mixing. We detected strong homophilic interactions between Flag- and HA-tagged Ten-m proteins and, to a lesser extent, between Flag- and HA-tagged Ten-a proteins (Fig. 5a). Ten-m and Ten-a also exhibited heterophilic interactions (Fig. 5a), which may account for their role in synapse organization[26].

Next, we tested whether Teneurins can homophilically promote *in vivo* trans-cellular interactions between PN dendrites and ORN axons. We simultaneously overexpressed Ten-m in Mz19 PNs using *Mz19-QF*, and Or67a and Or49a ORNs using *AM29-GAL4* (ref. 32; Fig. 5b). This enabled us to label and manipulate independently Mz19 dendrites and AM29 axons with distinct markers and transgenes. We chose *AM29-GAL4* because of its early onset of expression, whereas other class-specific ORN drivers start to express only after PN–ORN connection is established[5,6]. AM29 axons do not normally connect with Mz19 dendrites (Fig. 5c, d).

Simultaneous overexpression of Ten-m in both Mz19 PNs and AM29 ORNs produced ectopic connections between them (Fig. 5c, g), suggesting that Ten-m homophilically promotes PN–ORN attraction. By contrast, Ten-m overexpression only in PNs or ORNs did not produce any ectopic connections, despite causing dendrite or axon mistargeting, respectively (Fig. 5c, e, f). These data ruled out the involvement of heterophilic partners in Ten-m-mediated attraction. Simultaneous overexpression of Ten-a in Mz19 PNs and AM29 ORNs did not produce ectopic connections (data not shown), possibly due to lower expression or weaker Ten-a homophilic interactions (Fig. 5a). Although heterophilic interactions between Ten-m and Ten-a also occur *in vitro* (Fig. 5a), heterophilic overexpression of Ten-m and

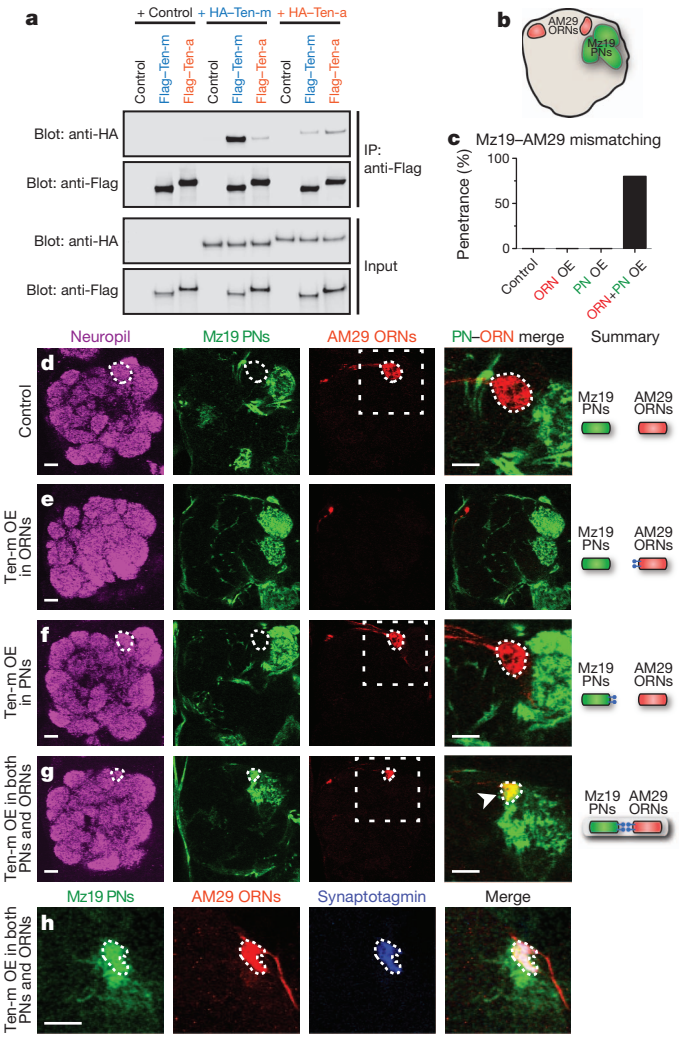

Figure 5 | Ten-m promotes homophilic interactions *in vitro* and *in vivo*. **a**, Co-immunoprecipitation of Flag- and HA-tagged Teneurin proteins from separately transfected S2 cells. Co-immunoprecipitated HA-tagged Teneurin proteins are detected by anti-HA antibody and immunoprecipitated Flag-tagged Teneurin proteins by anti-Flag antibody (top two blots). The input lysates are immunoblotted for HA and Flag (bottom two blots). **b**, Schematic showing the relative positions of glomeruli targeted by Mz19 PN dendrites (green) and AM29 ORN axons (red). **c**, Quantification of mismatching between Mz19 PNs and AM29 ORNs ($n = 10$ for each condition). OE, overexpression. **d**, In control, Mz19 dendrites do not connect with AM29 axons. **e**, **f**, Overexpression of Ten-m only in AM29 ORNs (**e**) or Mz19 PNs (**f**) does not produce mismatching between them. Following Ten-m overexpression, AM29 axons mistarget posteriorly to Mz19 dendrites and are therefore not visible in **e**. **g**, Simultaneous overexpression of Ten-m in both PNs and ORNs produces ectopic Mz19–AM29 connections (arrowhead). Schematics on the right show the Mz19–AM29 connectivity in different conditions. **h**, The synaptic vesicle marker Synaptotagmin is enriched at these Mz19–AM29 ectopic connections. AM29 axons are labelled by *AM29-Gal4* with *UAS-mtdT* to visualize the entire axonal processes and *UAS-synaptotagmin-HA* to visualize synaptic vesicles in axon terminals. Mz19 dendrites are labelled by *Mz19-QF* driving *QUAS-mCD8GFP*. To overexpress Ten-m, *P{GS}9267* and *QUAS-ten-m* (Supplementary Fig. 2) are driven by *AM29-GAL4* and *Mz19-QF*, respectively. Scale bars, 10 μm.

Ten-a in AM29 ORNs and Mz19 PNs did not produce ectopic connections (data not shown).

Finally, we examined whether these ectopic connections lead to the formation of synaptic structures. Indeed, the ectopic connections between Mz19 dendrites and AM29 axons were enriched in synaptotagmin–HA expressed from AM29 ORNs (Fig. 5h), suggesting that these connections can aggregate synaptic vesicles and could

be functional. We propose that Teneurins promote attraction between PN–ORN synaptic partners through homophilic interactions, eventually leading to synaptic connections.

Discussion

Compared to axon guidance, relatively little is known about synaptic target selection mechanisms[2–4]. Among the notable examples, the graded expressions of vertebrate EphA and ephrin-A instruct the topographic targeting of retinal ganglion cell axons[4,33–35]. Chick DSCAM and Sidekick promote lamina-specific arborization of retinal neurons[36]. *Drosophila* Capricious promotes target specificity of photoreceptor and motor axons[16,37–39]. *Caenorhabditis elegans* SYG-1 and SYG-2 specify synapse location through interaction between presynaptic axons and intermediate guidepost cells[40]. However, it is unclear whether any of these molecules mediate direct, selective interactions between individual pre- and postsynaptic partners. Indeed, in complex neural circuits, it is not clear a priori whether molecular determinants mediate such interactions. For example, the final retinotopic map is thought to result from both ephrin signalling and spontaneous activity[41,42]. Mammalian ORN axon targeting involves extensive axon–axon interactions through activity-dependent and independent modes[43,44], with minimal participation of postsynaptic neurons identified thus far.

Here, we show that Teneurins instruct PN–ORN matching through homophilic attraction. Although each glomerulus contains many synapses between cognate ORNs and PNs, these synapses transmit the same information and can be considered identical with regard to specificity. Thus, Teneurins represent a strong case in determining connection specificity directly between pre- and postsynaptic neurons. We further demonstrate that molecular determinants can instruct connection specificity of a moderately complex circuit at the level of individual synapses.

Our study reveals a requirement for PN–ORN attraction in the stepwise assembly of the olfactory circuit. PN dendrites and ORN axons first independently project to appropriate regions using global cues, dendrite–dendrite and axon–axon interactions[8,9,12–14]. The initial, independent targeting of PN dendrites and ORN axons is eventually coordinated in their final one-to-one matching. We identified Teneurins as the first molecules to mediate this matching process, through direct PN–ORN attraction. Our analyses have focused on a subset of PN–ORN pairs involving trichoid ORNs[45], including Or67d, Or88a and Or47b that have been implicated in pheromone sensation[46]. The partially overlapping expressions of Teneurins in other PN and ORN classes (Fig. 2 and Supplementary Fig. 4) suggest a broader involvement of Teneurins. At the same time, additional cell-surface molecules are also needed to determine completely connection specificity of all 50 PN–ORN pairs.

Teneurins are present throughout Animalia (Fig. 1h). Different vertebrate teneurins are broadly expressed in distinct and partially overlapping patterns in the nervous system[18]. Teneurin-3 is expressed in the visual system and is required for ipsilateral retinogeniculate projections[47]. Our study suggests that differential Teneurin expression may have a general role in matching pre- and postsynaptic partners. Indeed, high-level Ten-m is involved in matching select motor neurons and muscles[26]. Furthermore, Ten-m and Ten-a also trans-synaptically mediate neuromuscular synapse organization[26]. This suggests that the synapse partner matching function of Teneurins may have evolved from their basal role in synapse organization. Interestingly, synaptic partner matching only involves homophilic interactions (this study and ref. 26), whereas synapse organization preferentially involves heterophilic interactions[26]. This could not be fully accounted for by the different strength of their homophilic and heterophilic interactions *in vitro* (Fig. 5a). We speculate that these dual functions of Teneurins *in vivo* may engage signalling mechanisms that further distinguish homophilic versus heterophilic interactions.

METHODS SUMMARY

Detailed methods on fly stocks, generation of the *ten-a* allele, construction of transgenic flies, clonal analysis, histology, imaging, quantification and statistical analysis, epitope-tagged constructs, and co-immunoprecipitation can be found in Methods.

Full Methods and any associated references are available in the online version of the paper at www.nature.com/nature.

Received 14 June 2011; accepted 6 February 2012.
Published online 18 March 2012.

1. Sperry, R. W. Chemoaffinity in the orderly growth of nerve fiber patterns and connections. *Proc. Natl Acad. Sci. USA* **50,** 703–710 (1963).
2. Dickson, B. J. Molecular mechanisms of axon guidance. *Science* **298,** 1959–1964 (2002).
3. Zipursky, S. L. & Sanes, J. R. Chemoaffinity revisited: dscams, protocadherins, and neural circuit assembly. *Cell* **143,** 343–353 (2010).
4. Luo, L. & Flanagan, J. G. Development of continuous and discrete neural maps. *Neuron* **56,** 284–300 (2007).
5. Komiyama, T. & Luo, L. Development of wiring specificity in the olfactory system. *Curr. Opin. Neurobiol.* **16,** 67–73 (2006).
6. Brochtrup, A. & Hummel, T. Olfactory map formation in the *Drosophila* brain: genetic specificity and neuronal variability. *Curr. Opin. Neurobiol.* **21,** 85–92 (2011).
7. Jefferis, G. S. X. E. *et al.* Developmental origin of wiring specificity in the olfactory system of *Drosophila*. *Development* **131,** 117–130 (2003).
8. Komiyama, T., Sweeney, L. B., Schuldiner, O., Garcia, K. C. & Luo, L. Graded expression of semaphorin-1a cell-autonomously directs dendritic targeting of olfactory projection neurons. *Cell* **128,** 399–410 (2007).
9. Hong, W. *et al.* Leucine-rich repeat transmembrane proteins instruct discrete dendrite targeting in an olfactory map. *Nature Neurosci.* **12,** 1542–1550 (2009).
10. Hummel, T. *et al.* Axonal targeting of olfactory receptor neurons in *Drosophila* is controlled by Dscam. *Neuron* **37,** 221–231 (2004).
11. Hummel, T. & Zipursky, S. L. Afferent induction of olfactory glomeruli requires N-cadherin. *Neuron* **42,** 77–88 (2004).
12. Sweeney, L. B. *et al.* Temporal target restriction of olfactory receptor neurons by Semaphorin-1a/PlexinA-mediated axon-axon interactions. *Neuron* **53,** 185–200 (2007).
13. Lattemann, M. *et al.* Semaphorin-1a controls receptor neuron-specific axonal convergence in the primary olfactory center of *Drosophila*. *Neuron* **53,** 169–184 (2007).
14. Chou, Y.-H., Zheng, X., Beachy, P. A. & Luo, L. Patterning axon targeting of olfactory receptor neurons by coupled Hedgehog signaling at two distinct steps. *Cell* **142,** 954–966 (2010).
15. Zhu, H. *et al.* Dendritic patterning by Dscam and synaptic partner matching in the *Drosophila* antennal lobe. *Nature Neurosci.* **9,** 349–355 (2006).
16. Kurusu, M. *et al.* A screen of cell-surface molecules identifies leucine-rich repeat proteins as key mediators of synaptic target selection. *Neuron* **59,** 972–985 (2008).
17. Tucker, R. P. & Chiquet-Ehrismann, R. Teneurins: a conserved family of transmembrane proteins involved in intercellular signaling during development. *Dev. Biol.* **290,** 237–245 (2006).
18. Tucker, R. P., Kenzelmann, D., Trzebiatowska, A. & Chiquet-Ehrismann, R. Teneurins: transmembrane proteins with fundamental roles in development. *Int. J. Biochem. Cell Biol.* **39,** 292–297 (2007).
19. Young, T. R. & Leamey, C. A. Teneurins: important regulators of neural circuitry. *Int. J. Biochem. Cell Biol.* **41,** 990–993 (2009).
20. Baumgartner, S. & Chiquet-Ehrismann, R. *Ten*^{a}, a *Drosophila* gene related to tenascin, shows selective transcript localization. *Mech. Dev.* **40,** 165–176 (1993).
21. Baumgartner, S., Martin, D., Hagios, C. & Chiquet-Ehrismann, R. Tenm, a *Drosophila* gene related to tenascin, is a new pair-rule gene. *EMBO J.* **13,** 3728–3740 (1994).
22. Psychiatric GWAS Consortium Bipolar Disorder Working Group. Large-scale genome-wide association analysis of bipolar disorder identifies a new susceptibility locus near *ODZ4*. *Nature Genet.* **43,** 977–983 (2011).
23. Levine, A. *et al. odd Oz*: a novel *Drosophila* pair rule gene. *Cell* **77,** 587–598 (1994).
24. Zheng, L. *et al. Drosophila* Ten-m and Filamin affect motor neuron growth cone guidance. *PLoS ONE* **6,** e22956 (2011).
25. Liebl, F. L. W. *et al.* Genome-wide *P*-element screen for *Drosophila* synaptogenesis mutants. *J. Neurobiol.* **66,** 332–347 (2006).
26. Mosca, T. J., Hong, W., Dani, V. S., Favaloro, V. & Luo, L. Trans-synaptic Teneurin signalling in neuromuscular synapse organization and target choice. *Nature* http://dx.doi.org/10.1038/nature10923 (this issue).
27. Li, H., Bishop, K. M. & O'Leary, D. D. M. Potential target genes of EMX2 include *Odz/Ten-M* and other gene families with implications for cortical patterning. *Mol. Cell. Neurosci.* **33,** 136–149 (2006).
28. Rubin, B. P., Tucker, R. P., Brown-Luedi, M., Martin, D. & Chiquet-Ehrismann, R. Teneurin 2 is expressed by the neurons of the thalamofugal visual system *in situ* and promotes homophilic cell-cell adhesion *in vitro*. *Development* **129,** 4697–4705 (2002).
29. Oohashi, T. *et al.* Mouse Ten-m/Odz is a new family of dimeric type II transmembrane proteins expressed in many tissues. *J. Cell Biol.* **145,** 563–577 (1999).

30. Potter, C. J., Tasic, B., Russler, E. V., Liang, L. & Luo, L. The Q system: a repressible binary system for transgene expression, lineage tracing, and mosaic analysis. *Cell* **141,** 536–548 (2010).
31. Jefferis, G. S., Marin, E. C., Stocker, R. F. & Luo, L. Target neuron prespecification in the olfactory map of *Drosophila*. *Nature* **414,** 204–208 (2001).
32. Endo, K., Aoki, T., Yoda, Y., Kimura, K.-I. & Hama, C. Notch signal organizes the *Drosophila* olfactory circuitry by diversifying the sensory neuronal lineages. *Nature Neurosci.* **10,** 153–160 (2007).
33. Drescher, U. *et al. In vitro* guidance of retinal ganglion cell axons by RAGS, a 25 kDa tectal protein related to ligands for Eph receptor tyrosine kinases. *Cell* **82,** 359–370 (1995).
34. Cheng, H. J., Nakamoto, M., Bergemann, A. D. & Flanagan, J. G. Complementary gradients in expression and binding of ELF-1 and Mek4 in development of the topographic retinotectal projection map. *Cell* **82,** 371–381 (1995).
35. Feldheim, D. A. *et al.* Genetic analysis of ephrin-A2 and ephrin-A5 shows their requirement in multiple aspects of retinocollicular mapping. *Neuron* **25,** 563–574 (2000).
36. Yamagata, M. & Sanes, J. R. Dscam and Sidekick proteins direct lamina-specific synaptic connections in vertebrate retina. *Nature* **451,** 465–469 (2008).
37. Shinza-Kameda, M., Takasu, E., Sakurai, K., Hayashi, S. & Nose, A. Regulation of layer-specific targeting by reciprocal expression of a cell adhesion molecule, Capricious. *Neuron* **49,** 205–213 (2006).
38. Shishido, E., Takeichi, M. & Nose, A. *Drosophila* synapse formation: regulation by transmembrane protein with Leu-rich repeats, CAPRICIOUS. *Science* **280,** 2118–2121 (1998).
39. de Wit, J., Hong, W., Luo, L. & Ghosh, A. Role of leucine-rich repeat proteins in the development and function of neural circuits. *Annu. Rev. Cell Dev. Biol.* **27,** 697–729 (2011).
40. Shen, K., Fetter, R. D. & Bargmann, C. I. Synaptic specificity is generated by the synaptic guidepost protein SYG-2 and its receptor, SYG-1. *Cell* **116,** 869–881 (2004).
41. McLaughlin, T., Torborg, C. L., Feller, M. B. & O'Leary, D. D. M. Retinotopic map refinement requires spontaneous retinal waves during a brief critical period of development. *Neuron* **40,** 1147–1160 (2003).
42. Pfeiffenberger, C., Yamada, J. & Feldheim, D. A. Ephrin-As and patterned retinal activity act together in the development of topographic maps in the primary visual system. *J. Neurosci.* **26,** 12873–12884 (2006).
43. Imai, T. *et al.* Pre-target axon sorting establishes the neural map topography. *Science* **325,** 585–590 (2009).
44. Serizawa, S. *et al.* A neuronal identity code for the odorant receptor-specific and activity-dependent axon sorting. *Cell* **127,** 1057–1069 (2006).
45. Couto, A., Alenius, M. & Dickson, B. J. Molecular, anatomical, and functional organization of the *Drosophila* olfactory system. *Curr. Biol.* **15,** 1535–1547 (2005).
46. van der Goes van Naters, W. & Carlson, J. R. Receptors and neurons for fly odors in *Drosophila*. *Curr. Biol.* **17,** 606–612 (2007).
47. Leamey, C. A. *et al.* Ten_m3 regulates eye-specific patterning in the mammalian visual pathway and is required for binocular vision. *PLoS Biol.* **5,** e241 (2007).

Supplementary Information is linked to the online version of the paper at www.nature.com/nature.

Acknowledgements We thank V. Favaloro for advice on biochemistry and D. Luginbuhl for technical assistance; K. Zinn for the EP collection; H. Zhu for the initial contribution; R. Wides and S. Baumgartner for *teneurin* reagents; B. Zhang, Bloomington, Kyoto, Harvard and Vienna Stock Centers for fly stocks; BestGene for injection service; and K. Shen, T. Clandinin, D. Berns, V. Favaloro, X. Gao, S. Hippenmeyer, C. Liu, K. Miyamichi and X. Yu for critiques. Supported by a National Institutes of Health (NIH) grant (R01 DC-005982 to L.L.), and Epilepsy, Neonatology and Developmental Biology Training Grants (NIH 5T32 NS007280 and HD007249 to T.J.M.). L.L. is an investigator of the Howard Hughes Medical Institute.

Author Contributions W.H. designed and performed all experiments. T.J.M. assisted in some experiments. L.L. supervised the project. W.H. and L.L. wrote the manuscript with feedback from T.J.M.

Author Information Reprints and permissions information is available at www.nature.com/reprints. The authors declare no competing financial interests. Readers are welcome to comment on the online version of this article at www.nature.com/nature. Correspondence and requests for materials should be addressed to L.L. (lluo@stanford.edu).

METHODS

Fly stocks. *Mz19-GAL4* (ref. 7) was used to label PNs. *Or-rCD2* lines[15,48] (*Or47b-rCD2* and *Or88a-rCD2*), *Or-mCD8GFP* lines[45] (*Or23a-mCD8GFP*, *Or43a-mCD8GFP*, *Or46Aa-mCD8GFP*, *Or56a-mCD8GFP* and *Or83c-mCD8GFP*), *Or67d-GAL4* (ref. 49) and *AM29-GAL4* (ref. 32) were used to label ORNs. *GH146-Flp* (ref. 9), *ey-Flp* (ref. 50), *UAS>stop>mCD8GFP* (ref. 9) and *tubP>stop>GAL80* (ref. 51) were used to perform the intersectional expression analysis. *P{GS}9267* (*ten-m*) was generated by the *Drosophila* Gene Search Project (Metropolitan University)[52] and *P{GE}1914* (*ten-a*)[16] was from the GenExel collection of EP lines generated by the Korean Advanced Institute of Science and Technology. Their ability to drive the overexpression of each respective Teneurin was verified by elevated antibody staining.

All RNAi lines targeting *ten-m* or *ten-a* from the Vienna *Drosophila* RNAi Center (*UAS-ten-m*$^{RNAi\text{-}V51173}$ and *UAS-ten-a*$^{RNAi\text{-}V32482}$), the Bloomington *Drosophila* Stock Center (*UAS-ten-m*$^{RNAi\text{-}JF03323}$ and *UAS-ten-a*$^{RNAi\text{-}JF03375}$), and the National Institute of Genetics Fly Stock Center (*UAS-ten-m*$^{RNAi\text{-}5723R}$ and *UAS-ten-a*$^{RNAi\text{-}2590R}$) were collected. The efficiency of all RNAi lines was tested by pan-neuronal expression using *C155-GAL4* followed by Ten-m or Ten-a antibody staining. *UAS-ten-m*$^{RNAi\text{-}V51173}$ and *UAS-ten-m*$^{RNAi\text{-}JF03323}$ targeting *ten-m*, and *UAS-ten-a*$^{RNAi\text{-}V32482}$ and *UAS-ten-a*$^{RNAi\text{-}JF03375}$ targeting *ten-a* were able to eliminate respective antibody staining beyond detection. *UAS-ten-m*$^{RNAi\text{-}V51173}$ and *UAS-ten-a*$^{RNAi\text{-}V32482}$ were used in all the experiments except Supplementary Fig. 6, in which *UAS-ten-m*$^{RNAi\text{-}JF03323}$ and *UAS-ten-a*$^{RNAi\text{-}JF03375}$ were used to confirm the RNAi phenotypes. *UAS-Dcr2* (ref. 53) was used to enhance RNAi efficiency.

To identify *ten-m-GAL4*, we collected a group of GAL4 enhancer traps[54] located near the 5′ end of the *ten-m* gene. Their expression patterns were determined using a membrane-tagged GFP reporter *UAS-mCD8GFP* gene from the *Drosophila* Genetic Resource Center. *NP6658-GAL4*, which recapitulated the glomerulus-specific Ten-m staining pattern, was identified and referred to as *ten-m-GAL4*.

Generation of the *ten-a* allele. A small deficiency of *ten-a* was generated by FRT-mediated excision. This deficiency allele is homozygous viable and contains a deletion between *P{XP}d07540* and *PBac{WH}f01428*, which flanks the entire *ten-a* genomic region (~140 kb) and four additional predicted genes (Supplementary Fig. 2a), and is referred to as *Df(X)ten-a*. The deletion was verified by both PCR and antibody staining against Ten-a. The loss-of-function phenotypes were due to the loss of *ten-a* rather than the four additional predicted genes, as they mimicked the RNAi phenotypes.

Construction of *UAS* and *QUAS* transgenic flies. Ten-m and Ten-a coding sequences were amplified from the cDNA constructs[23,55,56]. One primer amplified from the start codon and added a CACC overhang for the TOPO reaction and a Kozak sequence. The other primer amplified to the stop codon. The PCR products were subcloned into *pENTR-D/TOPO* (Invitrogen). A 46-bp irrelevant fragment was found in the middle of the *ten-m* coding sequence in the original cDNA construct, and was removed by replacing a small region containing this fragment with the corresponding region in the *ten-m* genomic DNA. To make *UAS-ten-m*, *UAS-ten-a*, *QUAS-ten-m* and *QUAS-ten-a*, *pENTR-ten-m* and *pENTR-ten-a* were recombined into destination vector *pUASt-Gateway-attB*[57] and *pQUASt-Gateway-attB* using LR Clonase II (Invitrogen). The destination vector *pQUASt-Gateway-attB* was constructed by replacing the UAS site in *pUASt-Gateway-attB* with a QUAS site. All constructs were sequence verified. All the UAS and QUAS transgenes were integrated into both *attP24* and *86Fb* landing sites[58,59] on second and third chromosomes, respectively. All transgenic flies were verified by PCR and overexpression followed by antibody staining. The UAS and QUAS transgenes inserted in the *86Fb* site were used in this paper.

BAC recombineering to construct *Mz19-QF*. A 110-kb BAC (#CH321-85L03) in the *attB-P[acman]-CmR* vector[60], which contains genomic DNA that covers the *Mz19-GAL4* enhancer trap insertion site, was collected from the BACPAC Resources Center. The QF coding sequence, with a P-element minimal promoter and an hsp70 polyA, was amplified using primers containing 50-bp arm sequences allowing site-specific recombination. The 5-kb PCR product was recombined into the 110-kb genomic BAC using bacterial BAC recombineering and was verified by sequencing. The 115-kb Mz19-QF BAC was further verified by digestion pattern analysis and used to produce transgenes at the VK37 landing site[61] on the second chromosome by BestGene. The *Mz19-QF* transgenic flies were verified by PCR and the expression of reporters *QUAS-mCD8GFP* or *QUAS-mTdt3HA*.

Clonal analysis. To determine the contribution of individual PNs to the ectopic connections with ORNs, the MARCM method[62] was applied. Briefly, heat-shock-induced Flp activity caused mitotic recombination of the FRT chromosome arm such that one of the daughter cells lost *GAL80*. This cell (and its progeny) can therefore be labelled by the *GAL4-UAS* system. For generating neuroblast clones, flies were heat-shocked between 24–48 h after egg laying for 1 h at 37 °C. *Mz19-GAL4* labels VA1d and DC3 from the anterodorsal neuroblast and DA1 from the lateral neuroblast[7]. By generating neuroblast clones at 24–48 h after egg laying, we used *MZ19-GAL4* to specifically label DA1 or VA1d/DC3 PNs and simultaneously express RNAi targeting *ten-a*, or overexpress Ten-m or Ten-a in the labelled neurons.

In the *ten-a* mutant analysis, *Df(X)ten-a* was placed in *trans* to *GAL80* on the FRT chromosome arm. Upon Flp-induced mitotic recombination, one of the daughter cells became homozygous for *ten-a* and simultaneously lost *GAL80*. We used *MZ19-GAL4* to specifically label DA1 or VA1d/DC3 mutant PNs.

Different classes of ORNs, except for Or67d, were labelled by *Or-mCD8GFP* transgenes in a GAL4-independent manner, allowing the visualization of the specific matching between the labelled PNs and ORNs. Owing to the lack of an *Or67d-mCD8GFP*, Or67d ORNs were labelled by *Or67d-GAL4* and Ten-m overexpression was achieved by using *Mz19-QF* to drive *QUAS-ten-m* (Supplementary Fig. 9). In Teneurin overexpression by *Mz19-QF*, *Or67d-GAL4* expression was found unchanged compared with the control, and co-localized with Ncad staining in the DA1 glomerulus, which can be unambiguously identified (Supplementary Fig. 9). Therefore, Ncad staining in the DA1 glomerulus was used to determine the location of Or67d ORNs in Fig. 4f, l, in which Teneurins were overexpressed by *Mz19-GAL4*.

Histology. The procedures used for fixation and immunostaining were described previously[63]. For primary antibodies, we used mouse nc82 (1:30), rat antibody to N-cadherin (1:40), rat antibody to mCD8 (1:100), mouse antibody to rCD2 (1:200), chicken antibody to GFP (1:1,000), mouse antibody to HA (1:1,000), rabbit antibody to HA (1:1,000), rabbit antibody to DsRed (1:500), mouse antibody (mAb20) to Ten-m (1:3,000)[23], and guinea pig antibody to Ten-a (1:100)[64]. Neuropil staining indicates the antennal lobe, where PN dendrites and ORN axons are located. Fluorescent labelling outside the antennal lobe may come from labelled PN cell bodies or non-specific tissues.

Imaging, quantification and statistical analysis. Immunostained brains were imaged with a Zeiss LSM 510 Meta laser-scanning confocal microscope. Images of antennal lobes were taken as confocal stacks with 1-μm-thick sections. Representative single sections were shown to illustrate the matching and mismatching between PN dendrites and ORN axons. Penetrance of phenotypes represents the percentage of animals in which at least one antennal lobe showed a given phenotype among the total animals examined. Percentage of intermingling represents the fraction of labelled dendrites located within the axonal area of a given ORN class, and was measured by dividing dendritic area by total axonal area in a single confocal plane that shows maximum intermingling between dendrites and axons. Statistical significance between two samples was determined by the unpaired Student's *t*-test.

Flag- and HA-tagged constructs. To express Flag- and HA-tagged proteins in S2 cells, the Gateway destination vectors *pUASt-Flag-Gateway(-w)* and *pUASt-HA-Gateway(-w)* were generated by removing a ~4.5-kb non-essential fragment between two DraIII sites that contains the *white* gene from the original Gateway vectors pTFW and pTHW (*Drosophila* gateway collection, DGRC, Bloomington), respectively. The modified destination vectors are ~40% smaller than the original ones while preserving all the essential components for S2 cell expression, and showed greater transfection and expression efficiency in S2 cells. To express Flag- and HA-tagged Teneurin proteins in S2 cells, *pENTR-ten-m* and *pENTR-ten-a* were recombined into modified destination vectors *pUASt-Flag-Gateway(-w)* and *pUASt-HA-Gateway(-w)* using LR Clonase II (Invitrogen). All expression constructs, including *UAS-Flag-ten-m*, *UAS-Flag-ten-a*, *UAS-HA-ten-m* and *UAS-HA-ten-a*, were sequence verified.

Co-immunoprecipitation assay. S2 cells were cultured in Schneider's insect medium (Sigma) according to the manufacturer's description. *UAS-Flag-ten-m*, *UAS-Flag-ten-a*, *UAS-HA-ten-m* or *UAS-HA-ten-a* constructs were separately transfected into S2 cells, along with an *Actin5c-GAL4* vector, using the Effectene transfection reagent (QIAGEN). The amount of each construct and the number of cells used for transfection were adjusted to ensure comparable expression levels of Ten-m and Ten-a proteins. Three days after transfection, separately transfected cells were harvested, mixed together, and incubated for 1 h at room temperature (25 °C). Equivalent amounts of untransfected cells were used as controls, and the final mixtures contained the same total amount of cells under all co-immunoprecipitation conditions. The mixed cells were lysed in lysis buffer (50 mM Tris-HCl pH 7.4, 10 mM $MgCl_2$, 150 mM NaCl, 1 mM EGTA, 10% glycerol) supplemented with 0.5% Nonidet P-40 and protease inhibitor cocktail (Sigma). The cell lysates were then incubated with EZview Red anti-Flag M2 affinity gel (Sigma) for 3 h at 4 °C with rotation. The samples were washed extensively in lysis buffer. The proteins were eluted in 2% SDS elusion buffer, and were detected using western blot analysis using rat antibody to HA (1:1,000, Roche), mouse antibody to Flag (1:5,000, Sigma), and HRP-conjugated-goat antibodies to rat or mouse primaries (both at 1:20,000, Jackson ImmunoResearch)

48. Zhu, H. & Luo, L. Diverse functions of N-cadherin in dendritic and axonal terminal arborization of olfactory projection neurons. *Neuron* **42,** 63–75 (2004).

49. Kurtovic, A., Widmer, A. & Dickson, B. J. A single class of olfactory neurons mediates behavioural responses to a *Drosophila* sex pheromone. *Nature* **446,** 542–546 (2007).
50. Newsome, T. P., Asling, B. & Dickson, B. J. Analysis of *Drosophila* photoreceptor axon guidance in eye-specific mosaics. *Development* **127,** 851–860 (2000).
51. Bohm, R. A. *et al.* A genetic mosaic approach for neural circuit mapping in *Drosophila*. *Proc. Natl Acad. Sci. USA* **107,** 16378–16383 (2010).
52. Toba, G. *et al.* The gene search system. A method for efficient detection and rapid molecular identification of genes in *Drosophila melanogaster*. *Genetics* **151,** 725–737 (1999).
53. Dietzl, G. *et al.* A genome-wide transgenic RNAi library for conditional gene inactivation in *Drosophila*. *Nature* **448,** 151–156 (2007).
54. Hayashi, S. *et al.* GETDB, a database compiling expression patterns and molecular locations of a collection of Gal4 enhancer traps. *Genesis* **34,** 58–61 (2002).
55. Fascetti, N. & Baumgartner, S. Expression of *Drosophila* Ten-a, a dimeric receptor during embryonic development. *Mech. Dev.* **114,** 197–200 (2002).
56. Kinel-Tahan, Y., Weiss, H., Dgany, O., Levine, A. & Wides, R. *Drosophila odz* gene is required for multiple cell types in the compound retina. *Dev. Dyn.* **236,** 2541–2554 (2007).
57. Tea, J. S., Chihara, T. & Luo, L. Histone deacetylase Rpd3 regulates olfactory projection neuron dendrite targeting via the transcription factor Prospero. *J. Neurosci.* **30,** 9939–9946 (2010).
58. Markstein, M., Pitsouli, C., Villalta, C., Celniker, S. E. & Perrimon, N. Exploiting position effects and the gypsy retrovirus insulator to engineer precisely expressed transgenes. *Nature Genet.* **40,** 476 (2008).
59. Bischof, J., Maeda, R. K., Hediger, M., Karch, F. & Basler, K. An optimized transgenesis system for *Drosophila* using germ-line-specific ϕC31 integrases. *Proc. Natl Acad. Sci. USA* **104,** 3312–3317 (2007).
60. Venken, K. J. T. *et al.* Versatile P[acman] BAC libraries for transgenesis studies in *Drosophila melanogaster*. *Nature Methods* **6,** 431–434 (2009).
61. Venken, K. J. T., He, Y., Hoskins, R. A. & Bellen, H. J. P[acman]: a BAC transgenic platform for targeted insertion of large DNA fragments in *D. melanogaster*. *Science* **314,** 1747–1751 (2006).
62. Lee, T. & Luo, L. Mosaic analysis with a repressible cell marker for studies of gene function in neuronal morphogenesis. *Neuron* **22,** 451–461 (1999).
63. Wu, J. S. & Luo, L. A protocol for dissecting *Drosophila melanogaster* brains for live imaging or immunostaining. *Nature Protocols* **1,** 2110–2115 (2006).
64. Rakovitsky, N. *et al. Drosophila Ten-a* is a maternal pair-rule and patterning gene. *Mech. Dev.* **124,** 911–924 (2007).